Genetic deletion of JAM-C in pre-leukemic cells rewires leukemic stem cell gene expression program in AML

Julien M.P. Grenier, Céline Testut, Matthieu Bal, Florence Bardin, Maria de Grandis, Véronique Gelsi-Boyer, Julien Vernerny, Marjorie Delahaye, Samuel Granjeaud, Christophe Zemmour, et al.

REGULAR ARTICLE

blood advances

Genetic deletion of JAM-C in preleukemic cells rewires leukemic stem cell gene expression program in AML

Julien M. P. Grenier,[1,4] Céline Testut,[1] Matthieu Bal,[1,2] Florence Bardin,[1] Maria De Grandis,[3,4] Véronique Gelsi-Boyer,[1] Julien Vernerey,[1] Marjorie Delahaye,[1] Samuel Granjeaud,[1] Christophe Zemmour,[2] Jean-François Spinella,[5] Triantafyllos Chavakis,[6] Stéphane J. C. Mancini,[7] Jean-Marie Boher,[2] Josée Hébert,[8] Guy Sauvageau,[5] Norbert Vey,[1] Jürg Schwaller,[9] Marie-Anne Hospital,[10] Cyril Fauriat,[1] and Michel Aurrand-Lions[1]

[1]Aix Marseille University, CNRS, INSERM, Institut Paoli-Calmettes, CRCM, Equipe Labellisée Ligue 2020, Marseille, France; [2]Département de la Recherche Clinique et de l'Innovation, Institut Paoli-Calmettes, Marseille, France; [3]Aix-Marseille University, CNRS, EFS, ADES, Biologie des Groupes Sanguins, Marseille, France; [4]UMR 7268, Aix-Marseille Université, EFS, CNRS, GENGLOBE, Marseille, France; [5]Laboratory of Molecular Genetics of Stem Cells, Institute for Research in Immunology and Cancer, University of Montreal, Montreal, QC, Canada; [6]Institute for Clinical Chemistry and Laboratory Medicine, Faculty of Medicine, Technische Universität Dresden, Dresden, Germany; [7]UMR 1236, University of Rennes, INSERM, Etablissement Français du Sang Bretagne, Rennes, France; [8]Division of Hematology-Oncology, Department of Medicine, Maisonneuve-Rosemont Hospital, Université de Montréal, Montreal, QC, Canada; [9]Department of Biomedicine, University Children's Hospital, University of Basel, Basel, Switzerland; and [10]Département d'Hématologie, Institut Paoli-Calmettes, Marseille, France

Key Points

- The AP-1/TNF-α transcriptional program is upregulated in MLL-AF9–driven leukemic cells originating from JAM-C deleted mouse.
- Stratification of patients with AML using LSC score (LSC-17) is improved by the score associated with AP-1/TNF-α gene signature.

The leukemic stem cell (LSC) score LSC-17 based on a stemness–related gene expression signature is an indicator of poor disease outcome in acute myeloid leukemia (AML). However, it is not known whether "niche anchoring" of LSC affects disease evolution. To address this issue, we conditionally inactivated the adhesion molecule JAM-C (Junctional Adhesion Molecule-C) expressed by hematopoietic stem cells (HSCs) and LSCs in an inducible mixed-lineage leukemia (iMLL)-AF9–driven AML mouse model. Deletion of *Jam3* (encoding JAM-C) before induction of the leukemia–initiating iMLL-AF9 fusion resulted in a shift from long-term to short-term HSC expansion, without affecting disease initiation and progression. In vitro experiments showed that JAM-C controlled leukemic cell nesting irrespective of the bone marrow stromal cells used. RNA sequencing performed on leukemic HSCs isolated from diseased mice revealed that genes upregulated in *Jam3*-deficient animals belonged to activation protein-1 (AP-1) and tumor necrosis factor α (TNF-α)/NF-κB pathways. Human orthologs of dysregulated genes allowed to identify a score that was distinct from, and complementary to, the LSC-17 score. Substratification of patients with AML using LSC-17 and AP-1/TNF-α genes signature defined 4 groups with median survival ranging from <1 year to a median of "not reached" after 8 years. Finally, coculture experiments showed that AP-1 activation in leukemic cells was dependent on the nature of stromal cells. Altogether, our results identify the AP-1/TNF-α gene signature as a proxy of LSC anchoring in bone marrow niches, which improves the prognostic value of the LSC-17 score. This trial was registered at www.ClinicalTrials.gov as #NCT02320656.

Submitted 21 September 2023; accepted 19 June 2024; prepublished online on *Blood Advances* First Edition 2 July 2024; final version published online 30 August 2024. https://doi.org/10.1182/bloodadvances.2023011747.

Data sets have been deposited in the Gene Expression Omnibus database (accession number GSE235693).

All bioinformatic pipelines are available upon request from the corresponding author, Michel Aurrand-Lions (michel.aurrand-lions@inserm.fr).

The full-text version of this article contains a data supplement.

Introduction

Acute myeloid leukemia (AML) is a heterogeneous disease that originates from genetic alterations and clonal expansion of hematopoietic stem and progenitor cells (HSPCs). The organization of leukemic cells in AML is similar to normal hematopoiesis with leukemic stem cells (LSCs) at the apex that can reconstitute the clonal heterogeneity of AML disease in xenograft experiments.[1] LSCs are thought to be involved in AML relapse and enriched within, but not restricted to the $CD34^+/CD38^-$ phenotypic compartment.[2,3] Additional LSCs markers have thus been described including CD123, CD44, CLL1, CD96, CD47, TIM-3, CD32, CD25, IL1RAP, CD33, CD93, CD98, CD99, CD117, GPR56/ADGRG1, and JAM-C.[3-18] However, none of them, used alone or in combination, is necessary or sufficient to identify pure population of cells with leukemic initiating activity within or across patient samples, merely reflecting the heterogeneity of LSC in AML.[19,20] This prompted several teams to search for proxies reflecting the abundance of cells with leukemia-initiating activity that may predict disease outcome. Several gene expression signatures have been associated with poor prognosis[21-23] and some of them relied on increased frequencies of primitive quiescent LSCs in AML.[12,24-26] Among them, the leukemic stemness LSC-17 score represents 1 of the most robust LSC gene expression signatures, showing that the cellular hierarchy influences the overall characteristics of AML.[27] Other experimental approaches to identify hallmarks of LSCs comprised deciphering cellular heterogeneity of AML disease using single-cell RNA sequencing.[28-30] This allowed for the identification of differentially expressed genes (DEGs) in hematopoietic stem cell (HSC)–like cells as compared with more mature leukemic cells, some of which (*MMRN1*, *CD34*, *SOCS2*, *SMIM24*, *FAM30A*, and *CDK6*) are also included in the leukemic stemness LSC-17 score. Finally, modeling AML disease in mice identified features of leukemia-initiating cells.[31] Expression of the mixed-lineage leukemia *(MLL)-AF9* gene fusion induced transformation of HSPCs, which were able to reconstitute the disease.[32] Further studies using *Mll-AF9* heterozygous knockin mice[33] demonstrated that the most aggressive leukemia originated in HSCs rather than in more mature granulocyte/monocyte progenitors (GMPs).[34-36] More recently, study of the inducible MLL-AF9 (iMLL-AF9) model revealed that aggressiveness was correlated with high HSC expression of genes related to epithelial mesenchymal transition or cell adhesion.[37] This was consistent with our finding showing that human LSC ($CD45^{dim}CD34^+CD38^{low}CD123^+$) expressing the adhesion molecule JAM-C (Junctional Adhesion Molecule-C, encoded by JAM3) also expressed high levels of *ALCAM* or *ITGA6*, and that high frequency of JAM-C–expressing cells at diagnosis was associated with poor disease outcome.[4] These results suggest, but do not prove, that LSC adhesion to the surrounding bone marrow stromal cells (BMSCs) plays a role in AML disease initiation and outcome.

To model loss of LSC adhesion anchoring to BMSCs, we crossed conditional *Jam3*-deficient mice with the iMLL-AF9 leukemia model. Although *Jam3* deficiency did not delay disease evolution, we found upregulation of genes belonging to activation protein-1 (AP-1) and tumor necrosis factor α (TNF-α) pathways in *Jam3*-deleted LSCs as compared with control leukemic animals. Transposition of the results to the human disease allowed to define a new prognosis score called ATIC (AP-1/TNF-α initiating cells) that is complementary and distinct from the LSC-17 score.

Methods

Human samples

Human peripheral blood samples were collected with informed consent in the frame of NCT02320656 clinical trial according to the procedure approved by the institutional review board of Institut Paoli-Calmettes as sponsor of the study. Vials were thawed in, and thereafter washed in, RPMI 1640 containing 30% fetal calf serum (FCS), 1% penicillin/streptomycin, 100 U/mL DNase, and 10 U/mL of heparin. Dead cells were removed by layering 1 mL of cell suspension onto 2 mL of Ficoll followed by centrifugation for 20 minutes at 2000 RPM, after which cells were washed and maintained in RPMI 1640 containing 10% FCS and 1% penicillin/streptomycin until further use.

Mice experiments

iMLL-AF9 mice were crossed with Mx1-Cre *Jam3*$^{fl/fl}$ mice. *Jam3*$^{fl/fl}$ mice have been described previously.[38] All experiments were performed in compliance with the laws and protocols approved by animal ethics committees. Baseline white blood cell count (WBC) was assessed on day 0 in iMLL *Jam3*$^{fl/fl}$ mice, and *Jam3* gene deletion was induced by 3 intraperitoneal injections of 200 µg poly (I:C) (polyinosinic-polycytidylic acid; InvivoGen) on day 1, 3, and 5. Doxycycline (DOX; 400 µg/mL; Sigma) was provided in drinking water supplemented with 5% sucrose, 9 days after the last poly (I:C) injection. Leukemic burden was monitored weekly after WBC (ProCyte Dx Hematology Analyzer, IDEXX Laboratories).

Flow cytometry and cell sorting

Human samples were stained with antibodies described in supplemental Table 1 in phosphate-buffered saline containing 0.5 mM EDTA and 2% FCS (30 minutes at 4°C), washed, and processed for analysis. Mouse samples recovered from the femur and tibia were treated with 1× red blood cell lysing buffer (eBioscience) and stained with antibodies described in supplemental Table 1. Fluorescence-activated cell sorting analysis was performed on LSRII (BD Biosciences) or Aurora (Cytek). Cell sorting was performed using FACSAria III (BD Biosciences). Data were analyzed using DIVA version 8.01 (BD Biosciences) or OMIQ (OMIQ Inc).

RNA sequencing

HSCs and GMPs were directly sorted in RLT buffer from a messenger RNA (mRNA) purification kit using the RNeasy micro kit (QIAGEN). Samples were sent to the GenomEast platform (Illkirch, France). Libraries were paired-end sequenced (2 × 100 base pairs) on a Hiseq4000 system (Illumina).

Nanostring assay

Total mRNA from patient samples extracted using the RNeasy mini kit (QIAGEN) were hybridized with our custom nCounter Nanostring Code Set (supplemental Table 2) according to manufacturer instructions. Results were normalized using nSolver software (version 4.0), and $\log_2$ transformed values were used for LSC-17 score calculation.

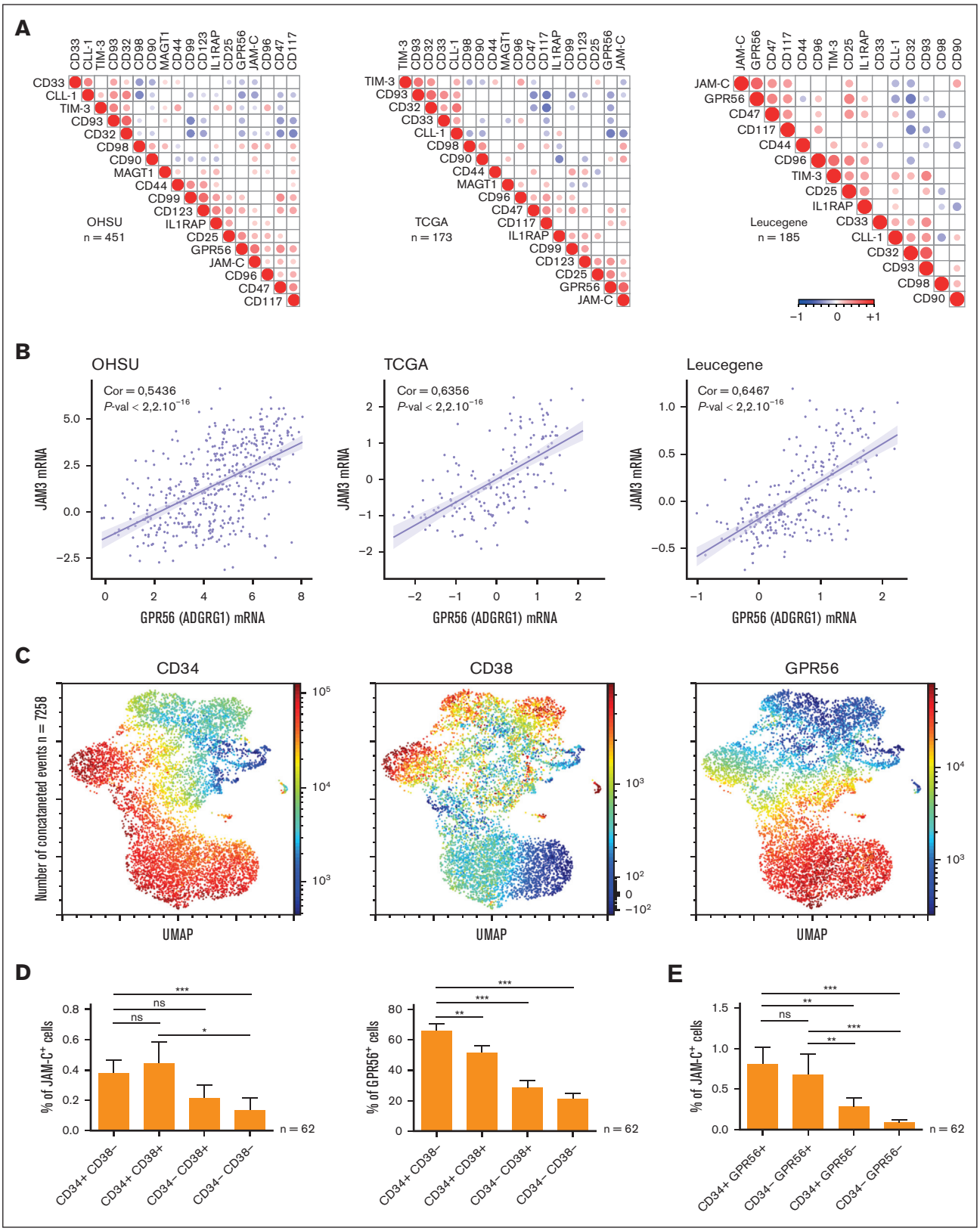

Figure 1. Expression of LSC markers in AML. (A) Pearson correlation analysis of genes encoding known AML LSC markers in 3 independent cohorts. Color and size represent the direction and the magnitude of the correlation, respectively. Only correlations with $P < .05$ are shown. (B) Scatter plots showing the relationship between *JAM3* and *GPR56* mRNA expression for individual samples of the indicated cohort. Pearson correlation and *P* value are shown. (C) Uniform manifold approximation and projection (UMAP)

Statistical analysis

Statistical analysis was performed using GraphPad 6 software and error bars represent the mean ± standard error of the mean. Normality was assayed using D'Agostino and Pearson omnibus normality test and samples were compared with a Mann-Whitney *U* test when normality was not reached. $*P < .05$; $**P < .01$; and $***P < .001$.

Publicly available data sets used for model training and validation

Publicly available mRNA sequencing data sets from the TCGA and OHSU cohort (also known as BEAT AML cohort[39]) were retrieved from cBioPortal using the CGDS-R package. The Leucegene data set was retrieved from Gene Expression Omnibus data repository (accession number GSE67040) and merged with clinical annotations. The 3 cohorts were assembled in a single matrix of gene expression, scaled, centered and half-split in training and validation cohorts. The ATIC score was established as the weighted sum of 14 gene expression as follow: ATIC score = (−0.02537109 × *JAM3*) + (−0.03654864 × *DUSP1*) + (−0.007206288 × *RGS1*) + (0.008025696 × *H2BC8*) + (−0.01143364 × *NFKBID*) + (−0.00423489 × *ZFP36*) + (−0.05511406 × *SLFN12*) + (−0.3608987 × *GAS5*) + (0.1012163 × *RPP25L*) + (0.05303331 × *HEY1*) + (−0.01449147 × *GIMAP4*) + (0.09348158 × *EFCAB11*) + (−0.03832157 × *CCL4*) + (−0.01028905 × *MYCN*). The gene expression data set from the HOVON/SAKK cohort (662 adult AML cases) was retrieved from the ArrayExpress database (accession number E-MTAB-3444) and gcrma maxVar expression values were used to calculate LSC-17 and ATIC scores.

Coculture experiments

For coculture experiments, 1×10^6 HS-5 or 8×10^5 HS-27 stromal cells were plated in 6-wells plates. Two days later, SKM1$^{JAM\text{-}C+}$ or SKM1$^{JAM\text{-}C-}$ cells were respectively labeled with calcein AM (C3100MP, ThermoFisher) and calcein red orange AM (C34851, ThermoFisher) for 30 minutes in phosphate-buffered saline, washed, mixed 1:1, and overlayed (2×10^6 cells) onto the stromal monolayers. After 7 hours of coculture, nonadherent, adherent, and nested cells were respectively collected by gentle aspiration, flushing, and trypsin digestion before analysis by flow cytometry. Leukemic cells were gated using CD45 staining (catalog no. 564357, BD) and results were expressed as ratios of calcein AM (SKM1$^{JAM\text{-}C+}$) and calcein red orange (SKM1$^{JAM\text{-}C-}$) cells.

Cell transduction

Lentiviral particles containing mock or AP-1–green fluorescent protein (GFP) reporter (TR411VA-P and TR452VA-P, respectively; System Biosciences) were transduced in SKM1$^{JAM\text{-}C+}$ or SKM1$^{JAM\text{-}C-}$. Cells were mixed with viral vectors at the multiplicity of infection of 10 (MOI 10) and 8 µg/mL of Polybrene before spinoculation at 1500*g* over 45 minutes. After 48 hours, transduced cells were selected with 0.6 µg/mL of puromycin for 7 days. AP-1 reporter expression was confirmed by stimulation with 20 ng/mL phorbol myristate acetate (PMA) for 24 hours, and analyzed by flow cytometry.

Results

JAM-C identifies a subset of LSCs

To address the phenotypic heterogeneity of LSCs, we conducted a correlation study of "LSC marker" gene expression across 3 cohorts of patients with AML (OHSU, TCGA, Leucegene).[39-41] Correlated expression between *GPR56* and *JAM-C* or *CD93* and *CD32* were systematically found, whereas correlation between other "LSC markers" varied from cohort to cohort (Figure 1A). We thus focused on GPR56 and JAM-C markers, which were highly significantly correlated (Figure 1B). Both markers were tested by flow cytometry in combination with live-dead, CD34, CD38, CD41, CD123, CD33, and CD45 in 62 blood samples from patients with AML (Table 1). Uniform manifold approximation and projection[42] analysis of JAM-C–expressing cells showed that most of the cells belonged to the CD34$^+$/GPR56$^+$/CD38$^{-/low}$ compartment (Figure 1C). Conversely, GPR56$^+$ cells expressed various levels of CD34, CD38, and JAM-C (supplemental Figure 1A), and higher frequencies of JAM-C$^+$/GPR56$^+$ cells were found in the CD34$^+$CD38$^{-/low}$ most-immature compartment (Figure 1D). JAM-C–expressing cells represented <1% of GPR56$^+$ cells and were almost absent from the most-mature CD34$^-$GPR56$^-$ compartment (Figure 1E). Because *GPR56* gene expression is contributing to the LSC-17 score, we tested whether *JAM3* expression was associated with the LSC-17 score. Results showed that *JAM3* (encoding JAM-C) and *GPR56* expression were significantly higher in samples belonging to the LSC-17^{High} group (supplemental Figure 1B).

Genetic deletion of JAM-C before leukemic onset alters HSPC expansion driven by iMLL-AF9 expression

To test whether JAM-C plays a role in the LSC transcriptional program, we established a mouse model in which conditional knock out of *Jam3* can be achieved before leukemic initiation. iMLL-AF9 mice were crossed with Mx1-Cre/*Jam3*$^{fl/fl}$ mice resulting in iMLL-AF9/Mx1-Cre/*Jam3*$^{fl/fl}$ mice (called iMLL *Jam3*$^{fl/fl}$ hereafter). Deletion of *Jam3* in hematopoietic cells was induced upon poly (I:C) injection, and AML was initiated by DOX-induced MLL-AF9.[37] Leukemia burden was measured by WBC and experiments were stopped when a value of 30 x 10^3 cells per µL was reached (Figure 2A; supplemental Figure 2A). JAM-C expression was not altered by leukemic transformation and efficient deletion of JAM-C in leukemic long-term (LT) HSCs (L-LT-HSCs), leukemic short-term (ST) HSCs (L-ST-HSC), and leukemic multipotent progenitors-3 (L-MPP-3) was observed upon poly (I:C) treatment (Figure 2B). *Jam3* deletion and loss of JAM-C protein expression were already achieved at the time of DOX induction, as shown by quantitative reverse transcription polymerase chain reaction and flow cytometry

Figure 1 (continued) plots of flow cytometry results showing expression of the indicated markers by JAM-C–expressing cells obtained from 62 concatenated samples; 7258 cells are shown. (D) Histogram showing the frequency of cells expressing JAM-C (left panel) or GPR56 (right panel) within the indicated phenotypic compartment defined by CD34 and CD38 expression. (E) Histogram showing the frequency of JAM-C–expressing cells within the indicated phenotypic compartment defined by combination of GPR56 and CD34 expression as described in Pabst et al.[17] Data are represented with mean ± standard error of the mean (SEM); ns, not significant; $*P < .05$; $**P < .01$; $***P < .001$.

Table 1. Flow cytometry sample characteristics

ID	Diagnosis	FAB	Karyotype	WBC (x10^9/L)
Patient no. 1	De novo	M4	47,XX,+8[20]	9.6
Patient no. 2	De novo	M2	46,XX,T(8;21)(Q22;Q22)[6]/ 46,IDEM,DEL(7)(Q21Q36)[13]/46,XX[1]	1.9
Patient no. 3	sAML (after MDS)	M1	Complex monosomal	15.1
Patient no. 4	De novo Relapse	M1	46,XX[20]	176.5
Patient no. 5	De novo	M2	47,XX,+11[4]/46,XX[16]	2.3
Patient no. 6	De novo	M1	46,XX[20]	86.3
Patient no. 7	De novo	M4	45,X,-Y,T(8;21)(Q22;Q22)[20]	44.9
Patient no. 8	De novo	M0	47,XY,+13[32]/46,XY[4]	1.4
Patient no. 9	sAML (after MDS)	M2	46,XY,DEL(5)(31Q35)[15]/47,IDEM,+14[3]/46,XY[7]	ND
Patient no. 10	De novo	M1	46,XX[20]	8.7
Patient no. 11	De novo	M2	46,XY[20]	1.5
Patient no. 12	De novo	M2	Complex monosomal	17.4
Patient no. 13	De novo	M4	46,XY[20]	7.3
Patient no. 14	De novo	M4	Complex monosomal	11.2
Patient no. 15	De novo	M2	46,XX,T(8;21)(Q22;Q22),T(11;17)(Q14;Q11-12)[20]	4.4
Patient no. 16	De novo	M2	47,XX,+8[4]/46,XX[20]	2.9
Patient no. 17	sAML (after MPN)	M0	46,XX,DEL(20)(Q11Q13)[2]/ 46,IDEM,DEL(7)(Q22Q32)[15]/46,XX[3]	23.8
Patient no. 18	De novo	NK	Complex monosomal	11.4
Patient no. 19	sAML (after MDS)	M1	46,XY[20]	59
Patient no. 20	De novo	NK	47,XY,+8[21]/46,XY[1]	1.3
Patient no. 21	De novo	M1	46,XY[20]	8.1
Patient no. 22	De novo	M0	NK	1
Patient no. 23	De novo	CMML	46,XY[20]	47.1
Patient no. 24	De novo	M1	46,XX,DEL(7)(Q22Q36)[20]	8.6
Patient no. 25	De novo	M4	Complex monosomal	10
Patient no. 26	De novo	M5	46,XY,ADD(17)(P1?3)[14]/46,XY[8]	35
Patient no. 27	De novo	NK	46,XY[20]	5.5
Patient no. 28	De novo	NK	46,XX[20]	0.5
Patient no. 29	De novo	M1	Complex	2.4
Patient no. 30	De novo	M1	47,XX,+10[37]/46,IDEM,DEL(9)(Q12Q32)[3]	136.9
Patient no. 31	De novo	M4	46,XY[20]	18.8
Patient no. 32	De novo	M0	46,XY[40]	185
Patient no. 33	De novo	M6	46,XY,INV(3)(Q21Q26)[20]	17.6
Patient no. 34	De novo	M5	Complex	80.2
Patient no. 35	De novo	M1	47,XX,+21[10]/46,XX[11]	6.7
Patient no. 36	De novo	M0	46,XY,?T(3;7;5)(P24;Q36;Q14)[20]	66
Patient no. 37	De novo	M0	46,XX[30]	2
Patient no. 38	De novo	M4	46,XY,INV(16)(P13Q22)[20]	29.7
Patient no. 39	sAML (after MDS)	M2	46,XY[20]	5.6
Patient no. 40	De novo	M2	46,XX[20]	3.2
Patient no. 41	De novo	M1	Complex monosomal	1
Patient no. 42	De novo	M0	45,XX,-7,DER(21)T(7;21)(P11;P11)[20]	2.8
Patient no. 43	De novo	M1	46,XX[20]	51.6
Patient no. 44	De novo	M4	Complex monosomal	23.4
Patient no. 45	De novo	M0	Complex monosomal	2.5

FAB, French-American-British classification; MDS, myelodysplastic syndrome; MPN, myeloproliferative neoplasm; NK, Not Known; ND, Not Determined; sAML, secondary AML.

Table 1 (continued)

ID	Diagnosis	FAB	Karyotype	WBC (x10^9/L)
Patient no. 46	De novo	M5	46,XY,T(9;11)(P21-22;Q23)[20]	169.9
Patient no. 47	sAML (after MPN)	M0	46,XY,DEL(7)(Q22Q36)[21]/46,IDEM,I(21)(Q10)[2]	5.2
Patient no. 48	De novo	M5	46,XY,T(6;9)(P22;Q34)[20]	41.8
Patient no. 49	De novo	M1	46,XX[20]	21.8
Patient no. 50	De novo	M5	46,XX,T(11;17)(Q23;Q12-21)[2]/47,IDEM,? DEL(11)(Q23 OR Q22Q24-)+21[20]	54.1
Patient no. 51	De novo	M2	46,XY[20]	3.32
Patient no. 52	De novo	M4	46,XX[20]	19.1
Patient no. 53	De novo	M2	46,XX[20]	3.9
Patient no. 54	De novo	M2	46,XY[20]	48.9
Patient no. 55	De novo	M2	46,XX[20]	6.9
Patient no. 56	De novo	NK	Complex monosomal	17.5
Patient no. 57	De novo	M5	47,XY,+21[21]/46,XY[1]	29
Patient no. 58	De novo	M2	45,XY,-7[3]/46,XY[17]	146
Patient no. 59	De novo	M4	Complex monosomal	2.5
Patient no. 60	Patient no. 14 relapse			
Patient no. 61	Patient no. 31 relapse			
Patient no. 62	Patient no. 40 relapse			

FAB, French-American-British classification; MDS, myelodysplastic syndrome; MPN, myeloproliferative neoplasm; NK, Not Known; ND, Not Determined; sAML, secondary AML.

(Figure 2C; supplemental Figure 2B). Similar WBC increase was observed in iMLL *Jam3*$^{ko/ko}$ or iMLL *Jam3*$^{fl/fl}$ leukemic mice as compared with nonleukemic animals (Figure 2D). Increase in red blood cells distribution width values, which preceded that of WBC as described in humans,[43] confirmed similar leukemia progression in *Jam3*–proficient and –deficient leukemic mice (Figure 2E).

Previous reports have shown that MLL-AF9–driven leukemia-initiating cells are found in the L-LT-HSC and leukemic GMP (L-GMP) compartments.[32,37,44] Early hematopoietic changes in nonleukemic and leukemic iMLL *Jam3*$^{fl/fl}$ and iMLL *Jam3*$^{ko/ko}$ mice was thus analyzed by flow cytometry using the gating strategy described in supplemental Figure 2C.[45] As previously reported,[37] we found a twofold reduction in the frequency of Lin$^-$Sca$^+$Kit$^+$ cells (LSK) in leukemic mice as compared with healthy animals regardless of JAM-C expression (Figure 2F). Within the LSK compartment, expansion of the L-LT-HSC compartment in diseased mice as compared with healthy controls was JAM-C dependent (Figure 2G). In contrast, expansion of the L-ST-HSC compartment observed in diseased animals was even further increased in *Jam3*–deficient leukemic mice, reaching >60% of the LSK compartment (Figure 2H). This was at the expense of L-MPP-2, -3 and -4 (supplemental Figure 2D). The twofold expansion of the L-GMP compartment observed in *Jam3*–proficient leukemic mice as compared with healthy animals was abolished in *Jam3*–deficient leukemic mice (Figure 2I). Uniform manifold approximation and projection analysis confirmed that expansion of L-LT-HSCs, L-ST-HSCs, and L-GMPs observed in iMLL-AF9 *Jam3*$^{fl/fl}$ mice was replaced by expansion of a common myeloid progenitor–like compartment in *Jam3*–deficient leukemic mice (Figure 2J; supplemental Figure 2E).

To avoid interindividual variability of leukemic onset (supplemental Figure 2A), we performed adoptive transfer experiments. Lethally irradiated recipients received transplantation with 10^6 bone marrow (BM) cells from noninduced naive iMLL-AF9 mice, and *Jam3* deletion was induced before or after DOX exposure. The first group received poly (I:C) 1 day after grafting and rested for 2 weeks before DOX induction, group: poly (I:C) -> DOX; whereas the second group was continuously treated with DOX starting on day 1 and received poly (I:C) after 2 weeks, group: DOX -> poly (I:C). We observed a trend toward faster progression of the disease in the group poly (I:C) -> DOX than in the DOX -> poly(I:C), with 3 of 4 mice reaching the end point after 7 weeks of DOX treatment. In contrast, the 3 mice from DOX -> poly (I:C) progressed after 10 weeks (supplemental Figure 3A-B). At end point, the nature of circulating blasts and infiltration of leukemic cells in the liver or spleen were similar between the groups (supplemental Figure 3C-F). In contrast, nonsupervized flow cytometry analysis of Lin$^-$Kit$^+$ (LK) HSPCs highlighted differences in BM content between the groups at end point. Nonleukemic, nonirradiated BM samples were included in the analysis as control. Unsupervised clustering revealed 6 clusters, with the clusters 1 to 5 being underrepresented in the DOX -> poly (I:C) group (Figure 3A). Clusters 1 to 5 contained LSKs whereas cluster 6 corresponded to LK cells lacking Sca-1 expression. L-LT-HSCs and L-ST-HSCs were respectively enriched in cluster 1 and 2, as illustrated by the expression profiles of Sca-1, CD150, CD135, CD48, and CD34 in these 2 clusters (Figure 3B). Clusters 3, 4, and 5 corresponded to MPP-2, MPP-3, and MPP-4, respectively. The proportion of cells in cluster 2, 3, and 4 was greatly increased in the poly (I:C) -> DOX group compared with DOX -> poly (I:C) indicating that deletion of JAM-C before leukemic induction has a profound effect on early steps of hematopoiesis. Finally, LK cells in the poly (I:C) -> DOX group showed a trend toward increased CD117 expression and reduced CD16/32 as compared with the DOX -> poly (I:C) group consistent with increased leukemic common myeloid progenitor–like expansion.

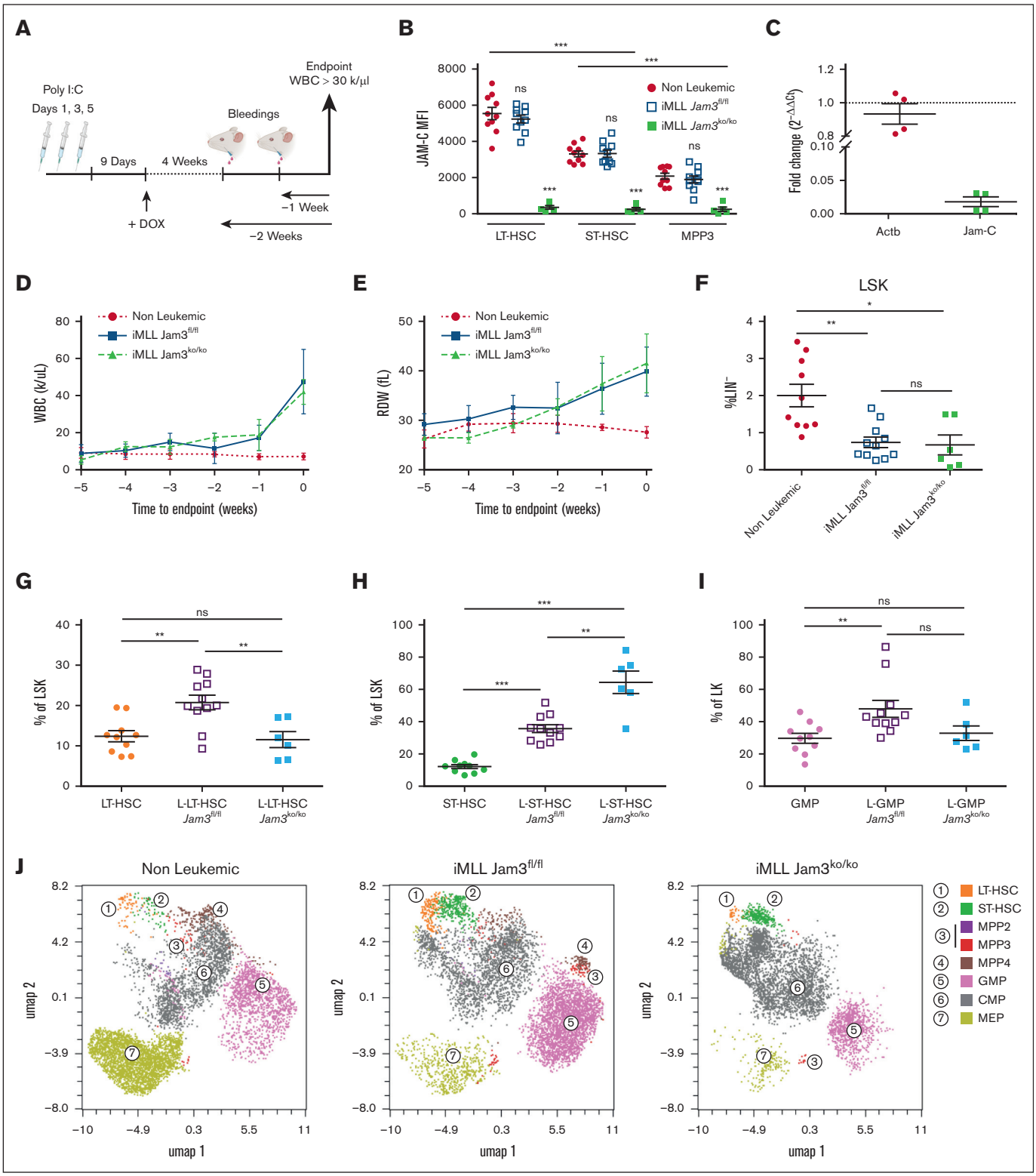

Figure 2. Conditional deletion of *Jam3* in HSPCs before leukemic onset exacerbates imbalanced hematopoiesis in an iMLL-AF9 mouse model. (A) Scheme illustrating the experimental procedure used for generation and analysis of conditional *Jam3*–deficient leukemic mice (iMLL $Jam3^{ko/ko}$), wild-type leukemic mice (iMLL $Jam3^{fl/fl}$), or nonleukemic control wild-type mice. (B) Graph showing the mean of fluorescence intensity (MFI) of JAM-C on indicated hematopoietic subsets isolated from the BM at end point. Results are shown for nonleukemic (filled circles), leukemic *Jam3*-proficient (empty squares), and *Jam3*-deficient animals (filled squares). (C) Graph showing the fold change in transcriptional expression of actin (*Actb*) and *Jam3*, 9 days after the last poly (I:C) injection at the time of leukemia induction with DOX. (D) Graph showing evolution of WBC in indicated group of animals. Time scale is normalized to end point. (E) Graph showing evolution of red cell distribution width (RDW) in indicated group of animals. (F-I) Graphs

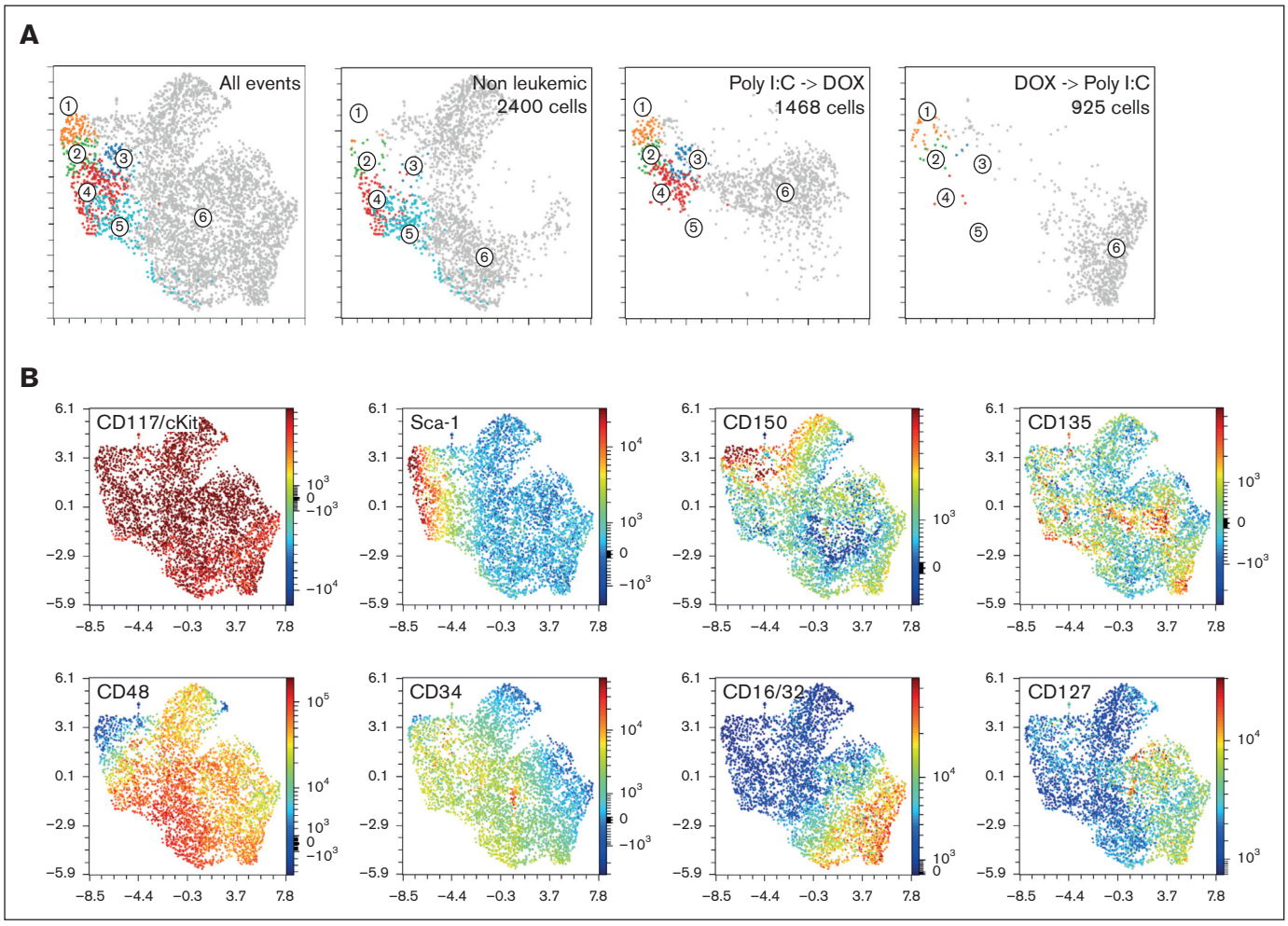

Figure 3. *Jam3* conditional deletion before or after leukemic onset changes proportions of leukemic stem and progenitor cells. (A) UMAP projection of Lin$^-$/c-Kit$^+$ cells isolated from nonleukemic engrafted mice (nonleukemic) and from grafted mice treated sequentially with poly (I:C) followed by DOX (poly (I:C) -> DOX group); or treated sequentially with DOX followed by poly (I:C), (Dox -> poly (I:C) group). Five clusters numbered 1 to 5 are identified (left panel) and shown for each of the indicated experimental conditions. The number of Lin$^-$/c-Kit$^+$ cells used for analysis is indicated. (B) Projection of the indicated marker expression on Lin$^-$/c-Kit$^+$ cells used to calculate the UMAP shown in panel A. Sca-1$^+$ compartment containing L-LT-HSCs and L-ST-HSCs belong essentially to clusters 1 and 2. Clusters 3 to 5 are Sca-1$^-$ and correspond to the LK compartment.

Jam3 deletion rewires the AP-1/TNF-α/NF-κB transcriptional network

To identify molecular mechanisms by which JAM-C regulates L-ST-HSC expansion, we performed bulk mRNA sequencing on L-HSCs (L-HSPC/CD48$^-$) and L-GMPs isolated from the BM of *Jam3*–proficient and *Jam3*–deficient diseased mice. All animals were treated with poly (I:C) before leukemia initiation by DOX. A total of 53 genes were upregulated in L-HSCs isolated from *Jam3*–deficient leukemic mice, whereas only 11 genes, including *Jam3,* were significantly downregulated (Figure 4A; supplemental Table 3). In L-GMPs isolated from *Jam3*–deficient leukemic mice, we also observed upregulated genes although the cells did not express JAM-C (Figure 4B).[46,47] Gene set enrichment analysis revealed enrichment of pathways related to cell-cell adhesion, TNF-α signaling via NF-κB and AP-1 transcription factor in L-HSCs isolated from leukemic *Jam3*-deficient mice (Figure 4C). The comparison of DEGs between *Jam3*–deficient and –proficient leukemic mice highlighted upregulation of several AP-1 family transcription factors including *Jun*, *Fos*, *Junb*, and *Jund* in leukemic L-HSCs and L-GMPs isolated from *Jam3*-deficient mice (Figure 4D; supplemental Figure 4). We then questioned whether genes affected by JAM-C deletion allow identification of specific LSC compartments in human AML. Notably, none of the DEGs

Figure 2 (continued) showing the relative frequencies of LSKs (F), LT-HSCs (G), ST-HSCs (H), and GMPs (I) isolated from the BM of nonleukemic (filled circles), leukemic *Jam3*-proficient (empty squares), and *Jam3*-deficient animals (filled squares). (J) UMAP projection of Lin$^-$/c-Kit$^+$/Sca-1$^{+/-}$ cells isolated from nonleukemic (left panel), iMLL *Jam3*$^{fl/fl}$ (middle panel), or iMLL *Jam3*$^{ko/ko}$ mice (right panel). Cell populations are color coded according to fluorescence-activated cell sorting gating and downsampling is adjusted to 2907 cells in all panels. Data are represented with mean ± SEM; ns, not significant; *$P < .05$; **$P < .01$; ***$P < .001$. CMP, common myeloid progenitor; MEP, megakaryocyte-erythrocyte progenitor; MPP, multipotent progenitor.

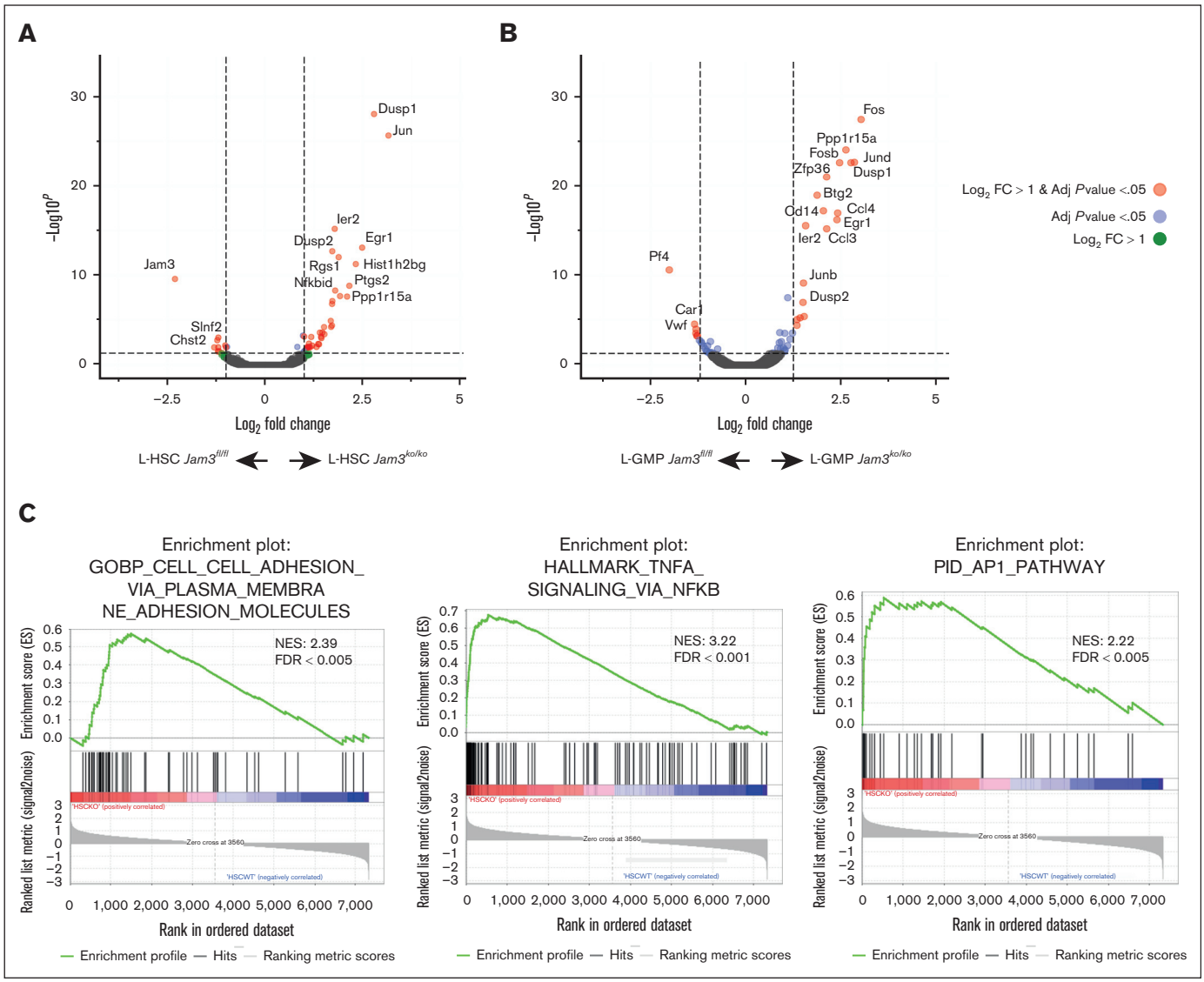

Figure 4. *Jam3* deficiency before leukemic onset upregulates AP-1/TNF-α transcriptional network in HSPCs. (A) Volcano plot displaying DEGs between L-HSCs isolated from the BM of *Jam3*–proficient (iMLL *Jam3*$^{fl/fl}$) and *Jam3*–deficient (iMLL *Jam3*$^{ko/ko}$) leukemic mice (n = 3 per genotype). The vertical axis shows the mean expression value of $\log_{10}$, and the horizontal axis shows the $\log_2$ fold change (FC) value obtained from triplicate experiments. Genes with $\log_2$ FC >1, and adjusted *P* value <.05, adjusted *P* value <.05 and $\log_2$ FC >1 are represented in red, blue, and green, respectively. (B) Volcano plot displaying DEGs for L-GMPs. (C) Gene set expression analysis using transcriptomes from L-HSCs shown in panel A. The most significant gene sets are shown. (D) Heat map showing $\log_2$ normalized transcripts per million (tpm) of genes differentially expressed between HSCs isolated from the BM of *Jam3*–deficient (iMLL *Jam3*$^{ko/ko}$) and *Jam3*–proficient (iMLL *Jam3*$^{fl/fl}$) leukemic mice (adjusted *P* < .05). Genes in gray are differentially expressed between *Jam3*-deficient and *Jam3*-proficient mice both in L-HSC and L-GMP compartments. (E) Venn diagram showing DEGs identified in this study, in the LSC-17 core signature,[24] or in genes defining the CD34$^+$/AP-1^{High} cluster in the single-cell RNA sequencing study by Velten et al.[28] FDR, false discovery rate; NES, net enrichment score.

identified in L-HSC and L-GMP iMLL-AF9 AML were present in the LSC-17 gene list (supplemental Table 4). In contrast, 25 of 56 DEGs found in our study were overexpressed by CD34$^+$ AP-1^{High} leukemic blasts previously identified by single-cell transcriptomic analysis of samples from patients with AML (Figure 4E).[28] Our observations suggest that JAM-C expression represses transcription of genes from AP-1 and TNF-α pathways that have been implicated in the transition between the preleukemic and leukemic stage.[48-50]

The AP-1/TNF-α signature substratifies patients with LSC-17 scores and identifies patients with AML with poor prognosis

To test whether the JAM-C–related differential AP-1/TNF-α signature may reflect a different cell of origin than those proposed by the LSC-17 or the Epithelial-Mesenchymal-Transition (EMT)-related gene expression signature of LT-HSC–derived iMLL-AF9 AML, gene expression correlation was carried out with 3 independent

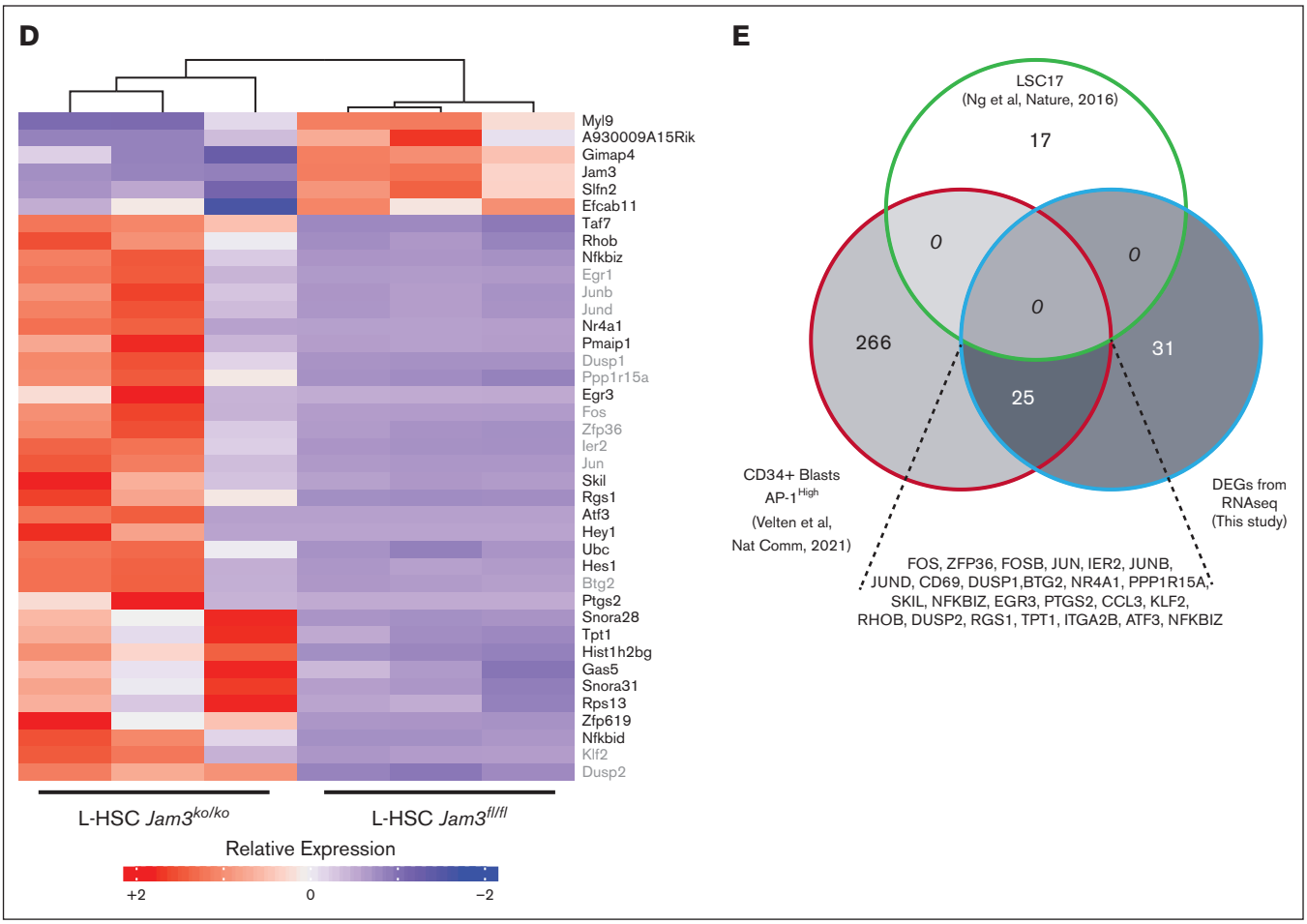

Figure 4 (continued)

AML cohorts (TCGA, Leucegene, and OHSU). Irrespective of the cohort, 2 major clusters of coregulated genes were identified and named cluster I and cluster II, respectively (Figure 5A; supplemental Figure 5). Cluster I contained *JAM3*, *ZEB1*, *ITGA6*, *ERG*, and genes from the LSC-17 score including *GPR56*, *DNMT3B*, and *NYNRIN* whereas genes belonging to the AP-1/TNF-α signature were mostly found in cluster II. Gene expression data sets from the 3 cohorts were thus assembled in a single mixed data set representing 871 patient samples to perform unsupervised clustering according to expression of genes from the LSC-17 score and AP-1/TNF-α DEG signature. Four groups of patients expressing inverse, high, or intermediate levels of the 2 gene expression signatures were identified (Figure 5B). This raised the question whether patients stratified by the LSC-17 score may be substratified by the AP-1/TNF-α DEG signature. To address this, the mixed data set was equally split in training and validation cohorts in order to define an ATIC score for LSC-17 substratification. We used the least absolute shrinkage and selection operator (LASSO) algorithm to relate expression of genes from the AP-1/TNF-α signature to patient survival in the training cohort using age and LSC-17 scores as offsets. LASSO was run on 2000 drawings of the training cohort. A weighted sum of gene expression obtained from the LASSO algorithm was fed into a Cox model to define a threshold for the ATIC score using either the maximally selected rank and statistics (Max-Stat) method or the median value of the ATIC score. Quality of the different models was then assessed according to the area under the curve, and accuracy of the 10 best models was tested with respect to median or Max-Stat thresholding. We found that most of the patients were classified as $ATIC^{High}$ or $ATIC^{Low}$ irrespective of the model (supplemental Figure 6; classification occurrence = 10). Only few patients were not repeatedly classified as high or low and had classification occurrence different from 10. Using median thresholding, 2 patients were classified 5 times as high and 5 times as low, resulting in a classification occurrence value of 0 (supplemental Figure 6A), whereas 4 patients belonged to the classification occurrence class 0 using Max-Stat thresholding (supplemental Figure 6B). We therefore chose median thresholding as the most robust method to calculate the ATIC score. Among the selected models, the model with the highest area under the curve and using genes detectable across all platforms (RNA sequencing, nCounter Nanostring, and Affymetrix) allowed us to define the ATIC score as the weighted sum of 14 genes (*JAM3*, *DUSP1*, *RGS1*, *H2BC8*, *NFKBID*, *ZFP36*, *SLFN12*, *GAS5*, *RPP25L*, *HEY1*, *GIMAP4*, *EFCAB11*, *CCL4*, and *MYCN*).

Combination of ATIC and LSC-17 scores identified patients with a median survival not reached after 8 years of follow-up in the $ATIC^{Low}$/LSC-17^{Low} arm (Figure 6A; supplemental Figure 6C),

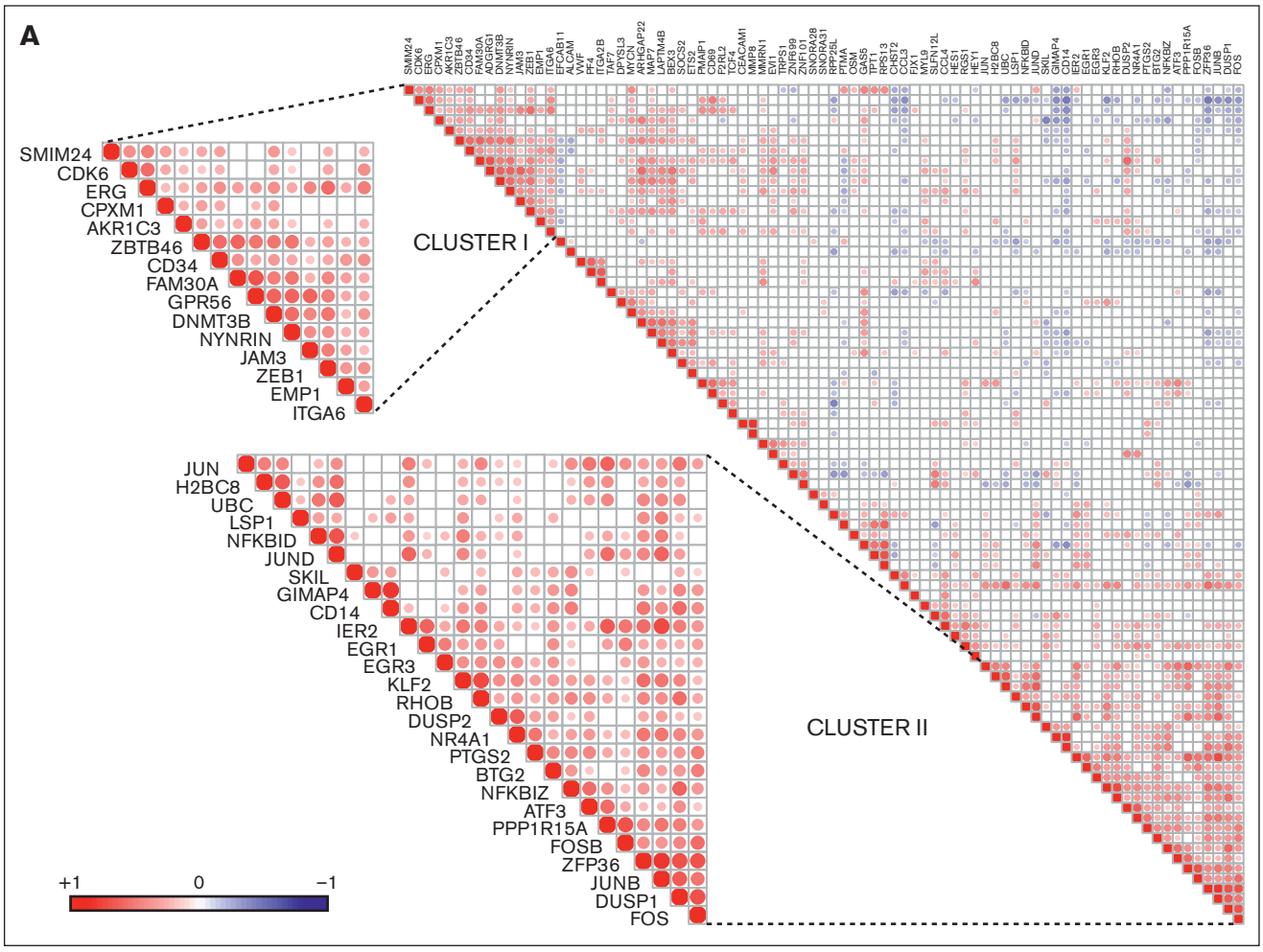

Figure 5. Genes from the LSC-17 score and AP-1/TNF-α signature belong to different clusters of coregulated genes in patients with AML. (A) Correlation plot showing expression of genes identified in this study and selected from Ng et al[24] and Stavropoulou et al[37] across samples from the TCGA cohort (n = 173). Color and size represent the direction and the magnitude of the correlation, respectively. Only correlations with $P < .05$ are shown. Two gene expression correlation clusters are underlined and conserved across cohorts (see also supplemental Figure 4). One cluster encompasses genes related to cell adhesion or migration (*ITGA6*, *ZEB1*, and *JAM3*) and genes from the LSC-17 score (cluster I). The second cluster contains number of genes upregulated in HSPCs isolated from *JAM3*–deficient leukemic mice (cluster II). (B) Heat map showing unsupervised patient sample clustering according to z score of genes belonging to the LSC-17 signature and DEGs from this study (supplemental Table 4) across samples from assembly of TCGA, OHSU, and Leucegene cohorts representing 871 AML samples at diagnosis. Four groups of samples can be visualized expressing respectively high or low levels of LSC-17 genes and high or low levels of DEGs identified in this study (AP-1/TNF-A1 signature). Groups of samples are underlined by red, black, green, and gray squares, respectively.

whereas patients belonging to the ATIC^{High}/LSC-17^{High} had a median survival of <1 year. To confirm these results, we tested an independent cohort of 662 adult AML cases for which gene expression was measured using Affymetrix (HOVON cohort). ATIC and LSC-17 scores were significantly associated with disease outcome and respective median survival of 12.3 months for LSC-17^{High}, 132 months for LSC-17^{Low}, 17.1 months for ATIC^{High}, and 31.1 months for ATIC^{Low} (supplemental Figure 6D-E). Despite the excellent predictive value of the LSC-17 score in this cohort, combination of the ATIC score with LSC-17 allowed us to reclassify 139 cases with ATIC^{High} score in each of the LSC-17 groups (Figure 6B). ATIC^{High}/LSC-17^{High} and ATIC^{Low}/LSC-17^{Low} scores were strongly associated with disease outcome with respective median survival values of 10.6 months and not reached after 200 months. The fact that the ATIC score was obtained from genes regulated upon JAM-C deletion in a mouse MLL-rearranged (MLLr) model called into question whether the ATIC score was specifically associated with known genetic classifiers of AML outcome such as MLLr, TP53 mutation, or other. In the OHSU cohort, patients with MLLr were enriched in the ATIC^{High}/LSC17^{Low} subgroup and associated with low expression of several stemness genes such as *KIAA0125*, *C19orf77*, *CPXM1*, *AKR1C3*, *CD34*, *JAM3*, or *GPR56* (Figure 6C). *CEBPA* mutations were exclusively found in the LSC17^{Low} group. *TP53*-mutated AML with myeloid-related changes were enriched in the LSC17^{High} group irrespective of ATIC score. Other AML with myeloid-related changes distributed across all 4 groups, similar to AML with *FLT3* and *NPM1* mutations.

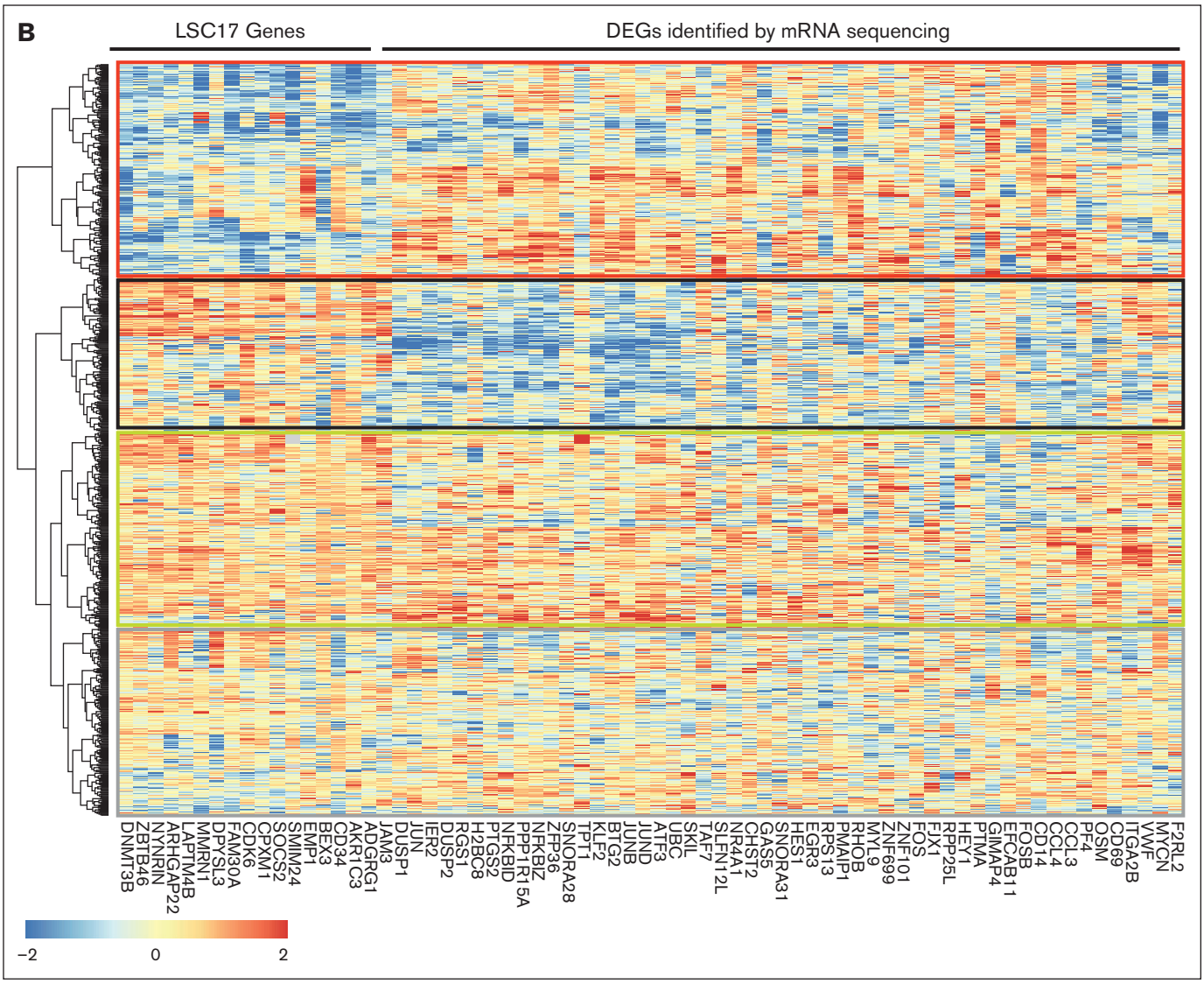

Figure 5 (continued)

BMSCs control AP-1 activation whereas JAM-C regulates leukemic cell nesting

Because the ATIC signature has been found after *Jam3* deletion in preleukemic cells and substratifies patients with different molecular alterations, our data suggest that the ATIC score reveals stromal cell–dependent disease heterogeneity. To test the functional consequences of JAM-C expression by leukemic cells, we isolated 2 isogenic variants from the parental SKM-1 AML cell line, which expressed JAM-C in a bimodal manner (supplemental Figure 7A). Adhesion of the 2 variant cell lines to the BM stromal cell lines HS-5 or HS-27 was tested upon coculture for 7 hours (supplemental Figure 7B). SKM-1$^{JAM\text{-}C+}$ cells were enriched in the nested fraction irrespective of the stromal cell line, indicating that JAM-C promotes leukemic cell retention under stromal cells (Figure 7A-B). To further explore whether JAM-C controls AP-1 activation, SKM-1 variant cell lines were transduced with AP-1 GFP reporter. Activation of AP-1 reporter cell lines with phorbol myristate acetate induced GFP expression irrespective of JAM-C expression (Figure 7C). Induction of the AP-1 GFP reporter was also observed upon coculture of reporter cells with the HS-5 stromal cell line irrespective of JAM-C expression (Figure 7D; supplemental Figure 7C). In contrast, the AP-1 GFP reporter was not induced upon coculture with the HS-27 cell line (Figure 7E; supplemental Figure 7C), indicating that AP-1 activation depends on the nature of the stromal cells.

Discussion

In this study, we explored the functional significance of JAM-C expression by leukemic subsets in AML. We found that JAM-C expression correlated with GPR56 and was enriched in the group of samples belonging to the LSC-17^{High} arm. This is consistent with previous findings showing that JAM-C and GPR56 identify human AML cells with high engraftment capacity.[4,17,51]

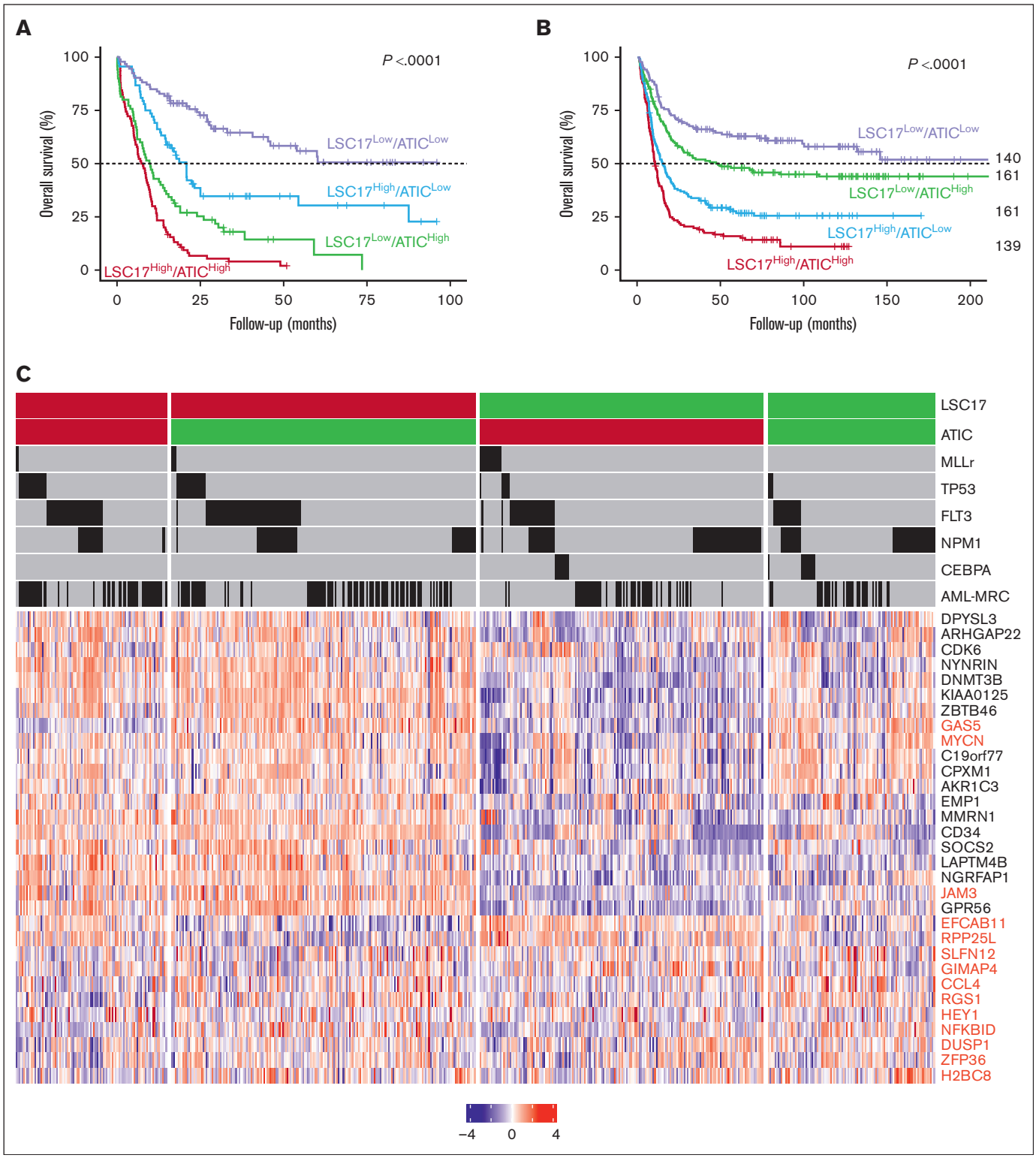

Figure 6. Risk stratification in AML according to LSC-17 and ATIC scores. (A) Kaplan-Meier survival curves of patients from the validation cohort according to combined stratification with LSC-17 and ATIC scores (n = 435). (B) Kaplan-Meier survival curves of patients from the HOVON/SAKK cohort (ArrayExpress, E-MTAB-3444) according to combined stratification with LSC-17 and ATIC scores (n = 600). Curve comparison *P* values are calculated by log-rank test. (C) Annotated heat map showing gene expression and known molecular alterations of patients from the OHSU cohort stratified with LSC-17 and ATIC scores. High and low scores are depicted in red and green, respectively. The presence of molecular alteration is shown by a black bar. Genes used to calculate LSC-17 and ATIC scores are shown in black and red, respectively.

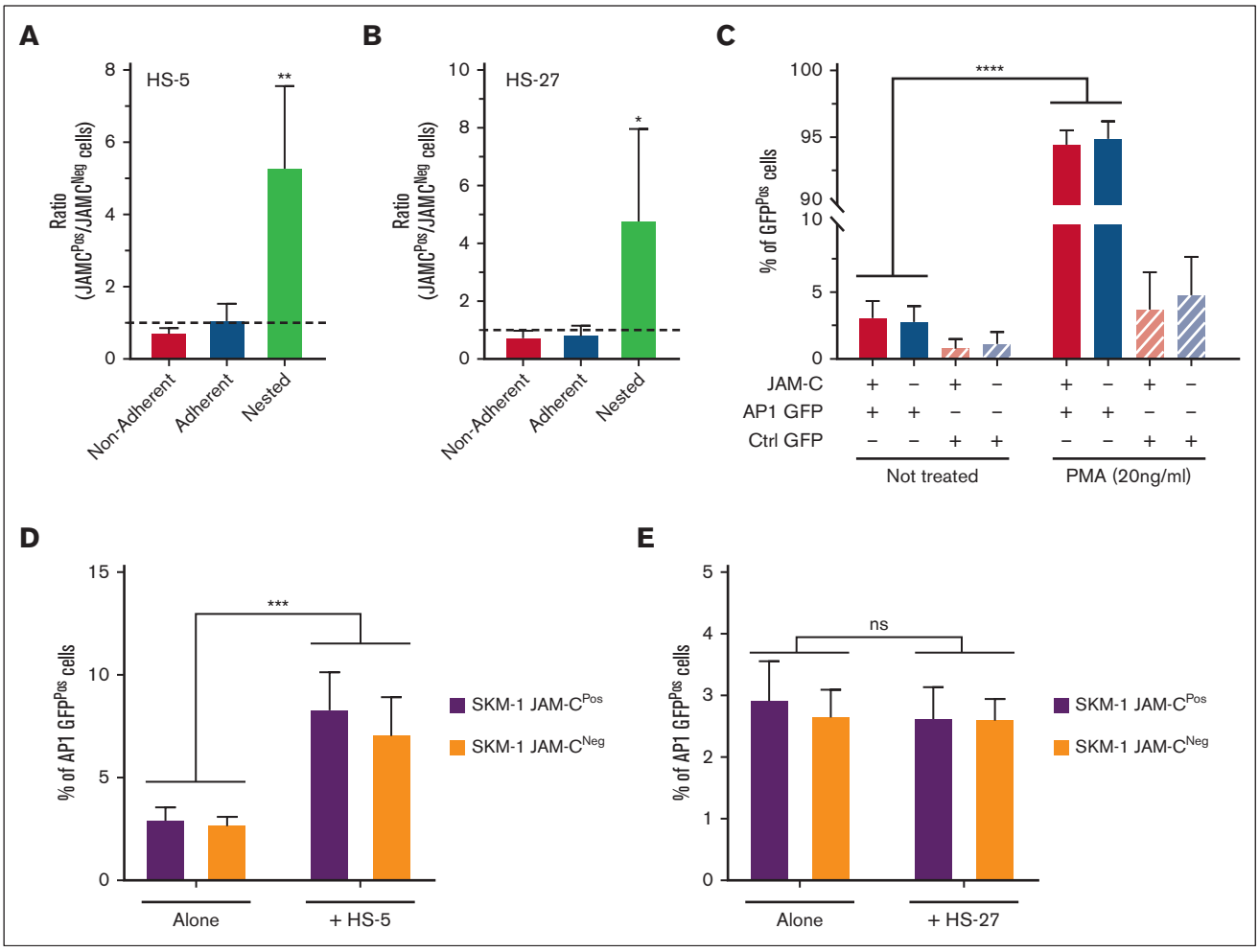

Figure 7. JAM-C is involved in leukemic cell nesting under stromal cells but does not directly control AP-1 activation. (A) Graph showing the repartition of SKM-1$^{JAM\text{-}C+}$ and SKM-1$^{JAM\text{-}C-}$ cells upon 7 hours of coculture with HS-5 stromal cells. (B) Graph showing the repartition of SKM-1$^{JAM\text{-}C+}$ and SKM-1$^{JAM\text{-}C-}$ cells upon 7 hours of coculture with HS-27 stromal cells. (C) Graph showing the percentage of GFP-expressing SKM-1$^{JAM\text{-}C+}$ (red) and SKM-1$^{JAM\text{-}C-}$ cells (blue) in absence of treatment and upon phorbol myristate actetate (PMA) activation. Variant cell lines were transduced with lentiviral constructs containing AP-1 GFP reporter (plain bars) or control (Ctrl) GFP reporter lacking AP-1 binding sites (dashed bars), as indicated. (D) Graph showing the percentage of GFP-expressing SKM-1$^{JAM\text{-}C+}$ (violet) and SKM-1$^{JAM\text{-}C-}$ cells (orange) in absence of coculture or after 7 hours of coculture with HS-5 stromal cells. (E) Graph showing the percentage of GFP-expressing SKM-1$^{JAM\text{-}C+}$ (violet) and SKM-1$^{JAM\text{-}C-}$ cells (orange) in absence of coculture or after 7 hours of coculture with HS-27 stromal cells. Data represent mean ± SEM from n = 3 independent experiments: ns, not significant; *$P < .05$; **$P < .01$; ***$P < .001$; ****$P < .0001$.

Enforced GPR56 expression has been shown to accelerate leukemogenesis of HOXA9-transduced hematopoietic cells, whereas silencing GPR56 expression delayed HOXA9/MEIS1-induced AML development.[52] However, this was independent of GPR56 binding to collagen III,[53] raising the question whether LSC adhesion to BM microenvironment was involved in LSC maintenance. Similarly, the function of JAM-C in leukemogenesis has been addressed through MLL-AF9 retroviral transduction of Jam3–proficient and Jam3–deficient progenitor cells.[54] Results showed that survival was slightly reduced in primary recipient mice receiving Jam3–deficient leukemic cells, whereas it was increased in serial transplants suggesting that JAM-C contributes to maintenance of LSC self-renewal. This was attributed to cell intrinsic signaling properties of JAM-C through its direct *cis* interaction with LRP5 because no defect in homing or adhesion to BMSCs was observed. However, these 2 studies required adoptive transfer and did not address the role of in situ adhesive properties of GPR56 or JAM-C at the time of leukemic transformation.

JAM-C is physiologically downregulated during normal hematopoiesis.[47,55,56] Therefore, we thought that JAM-C deletion before leukemic initiation may reveal changes in disease development or gene expression occurring when the first hit takes place in non-primitive HSC. *Jam3* deletion before MLL-AF9 expression in situ results in accumulation of L-ST-HSCs instead of L-LT-HSCs and L-GMPs.[37] Such phenotypic alterations are correlated with increased expression of AP-1/TNF-α genes, which has already been reported in CD34$^+$ AML blasts as compared with healthy HSPCs.[28,49] This suggests that the ATIC gene signature represents a proxy of the loss of preleukemic cell nesting in specific microanatomical sites and is consistent with the involvement of BMSCs in AP-1 activation in vitro. However, a major limitation of

our study is the lack of demonstration that preleukemic cell nesting is altered after JAM-C deletion at the time of leukemic initiation. Future studies using single-cell resolved spatial transcriptomics or proteomics should address this point.

A major finding of our study is the demonstration that the ATIC score allows substratification of patients classified with the LSC-17 score. Although the ATIC score was established based on an MLLr model in which we mimicked loosening of preleukemic cell adhesion to the niche, it allows substratification of patients with different mutational background. This raises the question whether the continuum between myeloproliferative neoplasm, myelodysplastic syndrome, and AML diseases relies on differential niche anchoring of preleukemic cells in specific microanatomical sites that can be detected by LSC-17 and ATIC scores.

Acknowledgments

The authors thank Manon Richaud and Françoise Mallet for invaluable help in flow cytometry analysis and cell sorting, Jean-Baptiste Marty for taking care of animal breeding and the CiBi core-facility for bioinformatic support. The authors thank P. Valk and M. Sanders for providing survival status for the HOVON/SAKK cohort.

This work has been supported by Ligue Nationale Contre le Cancer (Equipe labellisée 2020), Cancérôpole PACA, and Inca PRT-K16 (M.A.-L.) and GIRCI (M.A.-L. and M.-A.H.). J.M.P.G., and C.T. were supported by grants from the Société Française d'Hématologie. Generation of the iMLL-AF9 mouse model was supported by the Swiss National Science Foundation (SNF-31000A_173224, 2017-2020 [J.S.]).

Authorship

Contribution: J.M.P.G. performed experiments and wrote the manuscript; C.T., F.B., and M.D.G. performed experiments, and M.D. helped with mouse experiments; M.B., J.V., S.G., C.Z., J.-F.S., and J.-M.B. were in charge of bioinformatic analysis and data set processing; T.C. provided *Jam3*-floxed mice, and J.S. provided the iMLL-AF9 model; J.H. and G.S. provided clinical data from the Leucegene cohort; N.V. and M.-A.H. provided patient samples and clinical data from the NCT02320656 clinical trial; V.G.-B. interpreted clinical data, histological results, and blood smears; S.J.C.M. helped with interpretation of results; C.F. and M.A.L. were responsible for project supervision and coordination, experimental design, and manuscript preparation; all authors read and approved the manuscript.

Conflict-of-interest disclosure: The authors declare no competing financial interests.

ORCID profiles: M.D.G., 0000-0001-6465-8723; S.G., 0000-0001-9245-1535; C.Z., 0000-0002-8483-6117; J.-F.S., 0000-0003-2492-2897; J.H., 0000-0002-2267-1353; N.V., 0000-0001-7027-040X; J.S., 0000-0001-8616-0096; C.F., 0000-0002-4850-6831; M.A.-L., 0000-0002-8361-3034.

Correspondence: Michel Aurrand-Lions, Department of Onco-Haematology and Immuno-Oncology, Cancerology Research Center of Marseille, CRCM, INSERM UMR1068, CNRS UMR7258, Aix-Marseille Université U105, Institut Paoli-Calmettes, 27 Blvd Leï Roure, CS30059, Cedex 09, 13273 Marseille, France; email: michel.aurrand-lions@inserm.fr.

References

1. Bonnet D, Dick JE. Human acute myeloid leukemia is organized as a hierarchy that originates from a primitive hematopoietic cell. *Nat Med*. 1997;3(7):730-737.
2. Sarry J-E, Murphy K, Perry R, et al. Human acute myelogenous leukemia stem cells are rare and heterogeneous when assayed in NOD/SCID/IL2Rγc-deficient mice. *J Clin Invest*. 2011;121(1):384-395.
3. Lapidot T, Sirard C, Vormoor J, et al. A cell initiating human acute myeloid leukaemia after transplantation into SCID mice. *Nature*. 1994;367(6464):645-648.
4. De Grandis M, Bardin F, Fauriat C, et al. JAM-C identifies Src family kinase-activated leukemia-initiating cells and predicts poor prognosis in acute myeloid leukemia. *Cancer Res*. 2017;77(23):6627-6640.
5. Herrmann H, Sadovnik I, Eisenwort G, et al. Delineation of target expression profiles in CD34+/CD38- and CD34+/CD38+ stem and progenitor cells in AML and CML. *Blood Adv*. 2020;4(20):5118-5132.
6. Jordan CT, Upchurch D, Szilvassy SJ, et al. The interleukin-3 receptor alpha chain is a unique marker for human acute myelogenous leukemia stem cells. *Leukemia*. 2000;14(10):1777-1784.
7. Jin L, Hope KJ, Zhai Q, Smadja-Joffe F, Dick JE. Targeting of CD44 eradicates human acute myeloid leukemic stem cells. *Nat Med*. 2006;12(10):1167-1174.
8. van Rhenen A, van Dongen GAMS, Kelder A, et al. The novel AML stem cell associated antigen CLL-1 aids in discrimination between normal and leukemic stem cells. *Blood*. 2007;110(7):2659-2666.
9. Hosen N, Park CY, Tatsumi N, et al. CD96 is a leukemic stem cell-specific marker in human acute myeloid leukemia. *Proc Natl Acad Sci U S A*. 2007;104(26):11008-11013.
10. Jaiswal S, Jamieson CHM, Pang WW, et al. CD47 is upregulated on circulating hematopoietic stem cells and leukemia cells to avoid phagocytosis. *Cell*. 2009;138(2):271-285.
11. Kikushige Y, Shima T, Takayanagi S, et al. TIM-3 is a promising target to selectively kill acute myeloid leukemia stem cells. *Cell Stem Cell*. 2010;7(6):708-717.
12. Saito Y, Kitamura H, Hijikata A, et al. Identification of therapeutic targets for quiescent, chemotherapy-resistant human leukemia stem cells. *Sci Transl Med*. 2010;2(17):17ra9.

13. Askmyr M, Ågerstam H, Hansen N, et al. Selective killing of candidate AML stem cells by antibody targeting of IL1RAP. *Blood*. 2013;121(18):3709-3713.
14. Ehninger A, Kramer M, Röllig C, et al. Distribution and levels of cell surface expression of CD33 and CD123 in acute myeloid leukemia. *Blood Cancer J*. 2014;4(6):e218.
15. Iwasaki M, Liedtke M, Gentles AJ, Cleary ML. CD93 marks a non-quiescent human leukemia stem cell population and is required for development of MLL-rearranged acute myeloid leukemia. *Cell Stem Cell*. 2015;17(4):412-421.
16. Bajaj J, Konuma T, Lytle NK, et al. CD98-mediated adhesive signaling enables the establishment and propagation of acute myelogenous leukemia. *Cancer Cell*. 2016;30(5):792-805.
17. Pabst C, Bergeron A, Lavallée V-P, et al. GPR56 identifies primary human acute myeloid leukemia cells with high repopulating potential in vivo. *Blood*. 2016;127(16):2018-2027.
18. Chung SS, Eng WS, Hu W, et al. CD99 is a therapeutic target on disease stem cells in myeloid malignancies. *Sci Transl Med*. 2017;9(374):eaaj2025.
19. Ho T-C, LaMere M, Stevens BM, et al. Evolution of acute myelogenous leukemia stem cell properties after treatment and progression. *Blood*. 2016;128(13):1671-1678.
20. Taussig DC, Pearce DJ, Simpson C, et al. Hematopoietic stem cells express multiple myeloid markers: implications for the origin and targeted therapy of acute myeloid leukemia. *Blood*. 2005;106(13):4086-4092.
21. Wagner S, Vadakekolathu J, Tasian SK, et al. A parsimonious 3-gene signature predicts clinical outcomes in an acute myeloid leukemia multicohort study. *Blood Adv*. 2019;3(8):1330-1346.
22. Nehme A, Dakik H, Picou F, et al. Horizontal meta-analysis identifies common deregulated genes across AML subgroups providing a robust prognostic signature. *Blood Adv*. 2020;4(20):5322-5335.
23. Docking TR, Parker JDK, Jädersten M, et al. A clinical transcriptome approach to patient stratification and therapy selection in acute myeloid leukemia. *Nat Commun*. 2021;12(1):2474-2489.
24. Ng SWK, Mitchell A, Kennedy JA, et al. A 17-gene stemness score for rapid determination of risk in acute leukaemia. *Nature*. 2016;540(7633):433-437.
25. Gentles AJ, Plevritis SK, Majeti R, Alizadeh AA. Association of a leukemic stem cell gene expression signature with clinical outcomes in acute myeloid leukemia. *JAMA*. 2010;304(24):2706-2715.
26. Eppert K, Takenaka K, Lechman ER, et al. Stem cell gene expression programs influence clinical outcome in human leukemia. *Nat Med*. 2011;17(9):1086-1093.
27. Zeng AGX, Bansal S, Jin L, et al. A cellular hierarchy framework for understanding heterogeneity and predicting drug response in acute myeloid leukemia. *Nat Med*. 2022;28(6):1212-1223.
28. Velten L, Story BA, Hernández-Malmierca P, et al. Identification of leukemic and pre-leukemic stem cells by clonal tracking from single-cell transcriptomics. *Nat Commun*. 2021;12(1):1366-1379.
29. Wu J, Xiao Y, Sun J, et al. A single-cell survey of cellular hierarchy in acute myeloid leukemia. *J Hematol Oncol*. 2020;13(1):128-147.
30. van Galen P, Hovestadt V, Wadsworth Ii MH, et al. Single-cell RNA-seq reveals AML hierarchies relevant to disease progression and immunity. *Cell*. 2019;176(6):1265-1281.e24.
31. Fisher JN, Kalleda N, Stavropoulou V, Schwaller J. The impact of the cellular origin in acute myeloid leukemia: learning from mouse models. *HemaSphere*. 2019;3(1):e152.
32. Krivtsov AV, Twomey D, Feng Z, et al. Transformation from committed progenitor to leukaemia stem cell initiated by MLL-AF9. *Nature*. 2006;442(7104):818-822.
33. Dobson CL, Warren AJ, Pannell R, et al. The mll-AF9 gene fusion in mice controls myeloproliferation and specifies acute myeloid leukaemogenesis. *EMBO J*. 1999;18(13):3564-3574.
34. Chen W, Kumar AR, Hudson WA, et al. Malignant transformation initiated by Mll-AF9: gene dosage and critical target cells. *Cancer Cell*. 2008;13(5):432-440.
35. Krivtsov AV, Figueroa ME, Sinha AU, et al. Cell of origin determines clinically relevant subtypes of MLL-rearranged AML. *Leukemia*. 2013;27(4):852-860.
36. Bindels EMJ, Havermans M, Lugthart S, et al. EVI1 is critical for the pathogenesis of a subset of MLL-AF9-rearranged AMLs. *Blood*. 2012;119(24):5838-5849.
37. Stavropoulou V, Kaspar S, Brault L, et al. MLL-AF9 expression in hematopoietic stem cells drives a highly invasive AML expressing EMT-related genes linked to poor outcome. *Cancer Cell*. 2016;30(1):43-58.
38. Langer HF, Orlova VV, Xie C, et al. A novel function of junctional adhesion molecule-C in mediating melanoma cell metastasis. *Cancer Res*. 2011;71(12):4096-4105.
39. Tyner JW, Tognon CE, Bottomly D, et al. Functional genomic landscape of acute myeloid leukaemia. *Nature*. 2018;562(7728):526-531.
40. Liu J, Lichtenberg T, Hoadley KA, Poisson LM, Lazar AJ, Cherniack AD, Kovatich AJ, Benz CC, Levine DA, Lee AV, Omberg L, Wolf DM, Shriver CD, Thorsson V, Cancer Genome Atlas Research Network, Hu H. An integrated TCGA pan-cancer clinical data resource to drive high-quality survival outcome analytics. *Cell*. 2018;173(2):400-416.e11.

41. Lemieux S, Sargeant T, Laperrière D, et al. MiSTIC, an integrated platform for the analysis of heterogeneity in large tumour transcriptome datasets. *Nucleic Acids Res*. 2017;45(13):e122.
42. Becht E, McInnes L, Healy J, et al. Dimensionality reduction for visualizing single-cell data using UMAP. *Nat Biotechnol*. 2018;37(1):38-44.
43. Abelson S, Collord G, Ng SWK, et al. Prediction of acute myeloid leukaemia risk in healthy individuals. *Nature*. 2018;559(7714):400-404.
44. Somervaille TCP, Cleary ML. Identification and characterization of leukemia stem cells in murine MLL-AF9 acute myeloid leukemia. *Cancer Cell*. 2006; 10(4):257-268.
45. Pietras EM, Reynaud D, Kang Y-A, et al. Functionally distinct subsets of lineage-biased multipotent progenitors control blood production in normal and regenerative conditions. *Cell Stem Cell*. 2015;17(1):35-46.
46. Arcangeli M-L, Frontera V, Bardin F, et al. JAM-B regulates maintenance of hematopoietic stem cells in the bone marrow. *Blood*. 2011;118(17): 4609-4619.
47. Praetor A, McBride JM, Chiu H, et al. Genetic deletion of JAM-C reveals a role in myeloid progenitor generation. *Blood*. 2009;113(9):1919-1928.
48. Kellaway SG, Potluri S, Keane P, et al. Leukemic stem cells hijack lineage inappropriate signalling pathways to promote their growth. *Nat Commun*. 2024;15(1):1359-1381.
49. Assi SA, Imperato MR, Coleman DJL, et al. Subtype-specific regulatory network rewiring in acute myeloid leukemia. *Nat Genet*. 2019;51(1):151-162.
50. Assi SA, Bonifer C, Cockerill PN. Rewiring of the transcription factor network in acute myeloid leukemia. *Cancer Inform*. 2019;18(1): 1176935119859863.
51. von Bonin M, Moll K, Kramer M, et al. JAM-C expression as a biomarker to predict outcome of patients with acute myeloid leukemia-letter. *Cancer Res*. 2018;78(21):6339-6341.
52. Daria D, Kirsten N, Muranyi A, et al. GPR56 contributes to the development of acute myeloid leukemia in mice. *Leukemia*. 2016;30(8):1734-1741.
53. Luo R, Jeong S-J, Jin Z, Strokes N, Li S, Piao X. G protein-coupled receptor 56 and collagen III, a receptor-ligand pair, regulates cortical development and lamination. *Proc Natl Acad Sci U S A*. 2011;108(31):12925-12930.
54. Zhang Y, Xia F, Liu X, et al. JAM3 maintains leukemia-initiating cell self-renewal through LRP5/AKT/β-catenin/CCND1 signaling. *J Clin Invest*. 2018; 128(5):1737-1751.
55. Forsberg EC, Prohaska SS, Katzman S, Heffner GC, Stuart JM, Weissman IL. Differential expression of novel potential regulators in hematopoietic stem cells. *PLoS Genet*. 2005;1(3):281-294.
56. Arcangeli M-L, Bardin F, Frontera V, et al. Function of Jam-B/Jam-C interaction in homing and mobilization of human and mouse hematopoietic stem and progenitor cells. *Stem Cells*. 2014;32(4):1043-1054.